Single Cell Reactomics

Vasse, Gwenda F.; Buzon, Pedro; Melgert, Barbro N.; Roos, Wouter H.; van Rijn, Patrick

Published in:
Small methods

DOI:
10.1002/smtd.202000849

Publication date:
2021

small methods
www.small-methods.com

Single Cell Reactomics: Real-Time Single-Cell Activation Kinetics of Optically Trapped Macrophages

Gwenda F. Vasse, Pedro Buzón, Barbro N. Melgert, Wouter H. Roos,* and Patrick van Rijn**

Macrophages are well known for their role in immune responses and tissue homeostasis. They can polarize towards various phenotypes in response to biophysical and biochemical stimuli. However, little is known about the early kinetics of macrophage polarization in response to single biophysical or biochemical stimuli. Our approach, combining optical tweezers, confocal fluorescence microscopy, and microfluidics, allows us to isolate single macrophages and follow their immediate responses to a biochemical stimulus in real-time. This strategy enables live-cell imaging at high spatiotemporal resolution and omits surface adhesion and cell–cell contact as biophysical stimuli. The approach is validated by successfully following the early phase of an oxidative stress response of macrophages upon phorbol 12-myristate 13-acetate (PMA) stimulation, allowing detailed analysis of the initial macrophage response upon a single biochemical stimulus within seconds after its application, thereby eliminating delay times introduced by other techniques during the stimulation procedure. Hence, an unprecedented view of the early kinetics of macrophage polarization is provided.

1. Introduction

Macrophages are known to be versatile cells, playing an important role in innate immune responses as well as in tissue homeostasis. Traditionally, macrophages were divided into two main phenotypes based on their marker expression or function: M1 (classically activated or pro-inflammatory) or M2 (alternatively activated or anti-inflammatory).[1,2] However, in the past years, especially the single-cell omics technologies have led to the understanding that a whole spectrum of macrophage polarization states exists.[1,3,4] Many biochemical factors such as cytokines have been shown to influence the polarization state of macrophages and more recently the role of biophysical stimuli is gaining attention.[5–7] However, during experiments numerous biochemical and biophysical stimuli are present that can affect macrophage polarization. Macrophages are also known to be very heterogeneous cells and consequently their responses to any stimulus may differ from cell to cell.[8,9] Additionally, macrophages possess a high degree of plasticity and, therefore, their activation status after a stimulus largely depends on the time point studied.[10] This plasticity, sensitivity to stimuli, and heterogeneity of macrophages make it very challenging to study macrophage polarization properly.

The most common methods to study macrophage polarization are flow cytometry, immunohistochemistry, enzyme-linked immunosorbent assays, quantitative polymerase chain reaction (qPCR), and omics technologies.[11] Although these techniques contribute greatly to our understanding of macrophage activation, most of them have a low temporal resolution due to the time required for sample handling. In addition, for in vitro experiments, macrophages are attached to a stiff cell culture substrate during stimulation, which serves as an unnatural biophysical stimulus to them and

G. F. Vasse, Dr. P. van Rijn
Biomedical Engineering Department-FB40
W.J. Kolff Institute for Biomedical Engineering and Materials Science-FB41
University Medical Center Groningen
University of Groningen
Antonius Deusinglaan 1, Groningen 9713 AV, The Netherlands
E-mail: p.van.rijn@umcg.nl

The ORCID identification number(s) for the author(s) of this article can be found under https://doi.org/10.1002/smtd.202000849.

DOI: 10.1002/smtd.202000849

G. F. Vasse, Prof. B. N. Melgert
Department of Molecular Pharmacology
Groningen Research Institute for Pharmacy
University of Groningen
Antonius Deusinglaan 1, Groningen 9713 AV, The Netherlands
E-mail: b.n.melgert@rug.nl

G. F. Vasse, Prof. B. N. Melgert
GRIAC Research Institute
University Medical Center Groningen
University of Groningen
Hanzeplein 1, Groningen 9713 GZ, The Netherlands

P. Buzón, Prof. W. H. Roos
Moleculaire Biofysica
Zernike Instituut
University of Groningen
Nijenborgh 4, Groningen 9747 AG, The Netherlands
E-mail: w.h.roos@rug.nl

will likely interfere when studying the response to physiological biochemical stimuli. Therefore, in order to improve our understanding of macrophage polarization, we are in need of techniques that allow us to study the response of a single macrophage to a single biophysical or biochemical stimulus with high spatiotemporal resolution.

In this context, optical tweezers technology has proven its strength to study living cells at the single-cell level soon after its invention.[12,13] Particularly, its combination with fluorescence microscopy has proven very successful to perform surface-free measurements on eukaryotic cells.[14–16] Modern optical tweezers use highly focused laser beams to trap and manipulate objects in a noninvasive manner. It has been shown that optical trapping of monocytes occurs by their nucleus, the most condensed region of the cell, without compromising their viability for up to 1 h.[17] The main strengths of optical trapping rely on its ability to isolate and immobilize individual living cells while maintaining them in suspension.[14–18] Therefore, the biophysical stimuli coming from a surface are eliminated. These features are especially advantageous for the study of macrophages as they are known to show heterogeneous responses to a broad set of stimuli. Furthermore, the trapped cells can be exposed suddenly to different biochemical stimuli by using microfluidic systems, thus, eliminating the delay times introduced by other techniques during the stimulation procedure.

In this study, we applied a combination of optical tweezers, confocal fluorescence microscopy, and microfluidics to visualize macrophage activation with unprecedented spatiotemporal resolution. Optical trapping of the macrophages allows us to eliminate effects of surface adhesion and cell–cell interactions as biophysical stimuli, whereas the microfluidics facilitates controlled addition of biochemical factors. We demonstrate that this methodology enables the study of early macrophage activation kinetics at the single-cell level, allowing further elucidation of the initial mechanisms of macrophage responses. For the verification and validation of this new method, we studied the levels of reactive oxygen species (ROS) in optically trapped RAW264.7 macrophages upon activation with phorbol 12-myristate 13-acetate (PMA). Implementation of this technique in macrophage polarization research will allow studies of the very first responses, which are not achievable by any other technique, and thereby gain novel insights into the mechanisms involved in macrophage activation.

2. Results

2.1. Optically Trapped RAW264.7 Macrophages are Responsive and Viable

Single RAW264.7 macrophages were trapped by a dual-beam laser with a beam-to-beam distance of 2 μm (**Figure 1**a and Experimental Section). This configuration proved to reduce rotation of the cell within the optical trap and therefore to improve imaging quality.[16] Macrophages were consistently presenting a round shape, characteristic of cells that are in suspension (Figure 1a).

To investigate whether optically trapped macrophages are still responsive to stimuli, we activated the macrophages with PMA (a known inducer of ROS).[19,20] ROS levels were visualized using CellROX Deep Red Reagent, a non-fluorescent dye that becomes fluorescent upon oxidation by ROS. Cell viability was monitored using SYTOX Orange Nucleic Acid stain, impermeable to living cells. Both the cell viability and intracellular ROS levels were monitored continuously by confocal fluorescence microscopy for 20 min (Figure 1b–c). All PMA-activated macrophages showed a fast increase in ROS levels within 5 min after stimulation, whereas this significant increase was not observed in unstimulated macrophages (Figure 1d). After approximately 10 min and a more than two-fold increase in ROS levels (Figure 1e), ROS levels stabilized in the PMA-stimulated macrophages. The unstimulated macrophages showed a minor decrease in ROS levels over time, suggesting that the optical trap is not generating ROS in macrophages. From these results, we can conclude that optically trapped macrophages are still responsive to stimulation.

Cell viability was followed in real-time by imaging and quantifying the SYTOX signal and localization in every cell. We observed that the SYTOX signal was mostly found on the cell membrane and, to a lesser extent, in the cytosol (Figure 1b,c). Figure 1f shows the average fluorescent signal obtained for both the control and PMA-stimulated cells. We noticed that the stimulated macrophages showed an increase in SYTOX signal during the initial 5 min, in contrast to the slight decrease that was found for the nonstimulated cells. Control experiments carried out without CellROX staining suggested that the increasing SYTOX signal is due to emission cross-talk between the fluorescence detectors (Figure S1, Supporting Information). The CellROX signal was also detected in the green channel, while the SYTOX signal showed negligible bleed-through into the red channel (Figure S1, Supporting Information). As internal positive control for our viability assay, we damaged every trapped macrophage with a 2-min dose of high intensity trapping laser (≈10 W) at the end of each experiment. This treatment significantly increased the overall SYTOX signal, as compared to the signal recorded within the first 20 min and was mostly localized in the nucleus (Figure 1f). The differences found in SYTOX intensity and localization allowed us to clearly distinguish between live and dead cells. Our observations indicate that the mild laser intensities used for cell trapping are not affecting macrophage viability and thereby support the applicability of optical tweezers for live-cell studies.

2.2. High Spatiotemporal Resolution Visualizes ROS Localization in Trapped Macrophages

The high spatiotemporal resolution of the confocal fluorescence microscope provides further insights into the response mechanism of optically trapped macrophages upon PMA stimulation. **Figure 2**a shows representative images of a trapped macrophage during an activation experiment and the fluorescence intensity profiles obtained from a cross-section of the cytoplasm. The ROS signal clearly spread rapidly within the first few minutes and stabilized after approximately 6 min. Indeed, ROS expression was found to be distributed in clusters at the beginning of the experiment and new clusters appeared across different parts of the cell, eventually merging until the cytosol was fully occupied (Figure 2a, upper panel). The

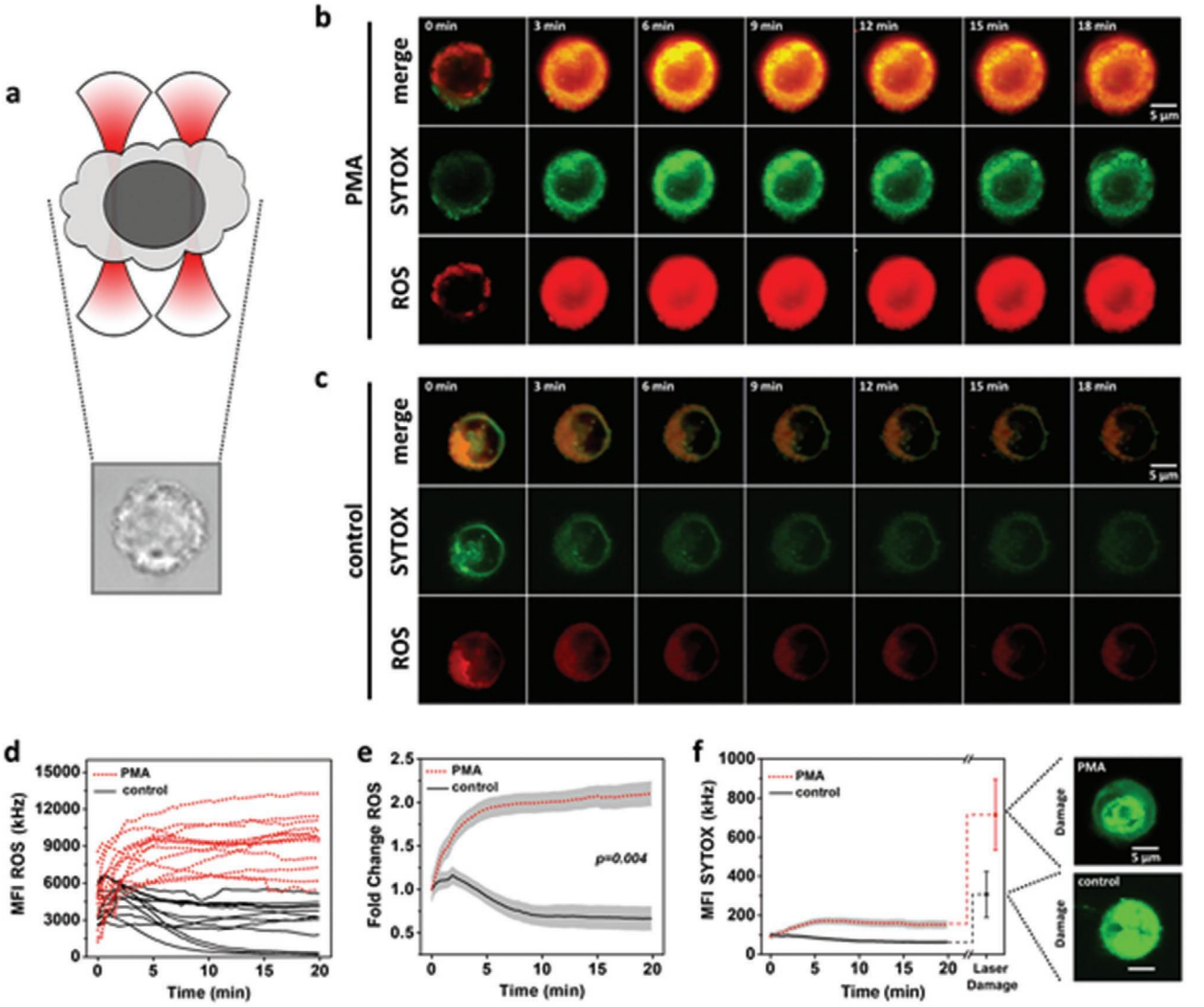

Figure 1. Responsiveness and viability of optically trapped RAW264.7 macrophages. a) A schematic representation of a macrophage immobilized by a dual-beam optical trap and a bright field image showing the round shape of an optically trapped macrophage. b) Time-lapse images of reactive oxygen species (ROS) (CellROX Deep Red) and SYTOX (green) signals in a trapped macrophage stimulated with phorbol 12-myristate 13-acetate (PMA). c) Time-lapse images of ROS (CellROX Deep Red) and SYTOX (green) signals in a trapped, unstimulated macrophage. The brightness in this panel is increased with respect to (b) for visualization purposes. d) ROS levels shown as mean fluorescence intensity measured in individual macrophages in the absence (black lines) or presence (red dotted lines) of PMA. e) Average fold change in ROS signal calculated from the single-cell curves shown in (d). Difference in area under the curve statistically tested with a Mann–Whitney *U* test ($p = 0.004$). f) Mean fluorescence intensity of SYTOX signals in PMA-stimulated cells (red dotted line) and controls (black line) during real-time imaging (up to 20 min) and after the cell is damaged by a 2-min dose of high intensity laser. The end points of the real-time imaging traces are connected to their respective laser damage point by dashed lines. Inserts on the right showing the localization of SYTOX in a stimulated and unstimulated macrophage after laser damage. Gray shades and error bars represent SEM for both PMA-stimulated ($N = 13$) and control ($N = 11$) macrophages.

cross-sectional intensity profiles presented in Figure 2a (lower panel) provide quantitative measurements that support these observations. The most dramatic changes in the overall intensity were found within the first 2 min, during which we also find the most heterogeneous fluorescent signal. Then, the ROS signal gradually became more homogeneous across the cytosol, remaining evenly distributed after 6 min.

In addition, we analyzed several morphological parameters that may be connected to these changes in ROS signal (see Figure 2b–d and Figure S2, Supporting Information). Cell contours were calculated by analyzing the distribution of ROS across the macrophages at different time points during the activation experiment (Figure 2b). Figure 2c shows the macrophage response to PMA activation in terms of changes in homogeneity of the fluorescence signal (see Experimental Section). This parameter gives information about the distribution of the signal within the area of interest, from 0 to 1, with 1 representing an ideally

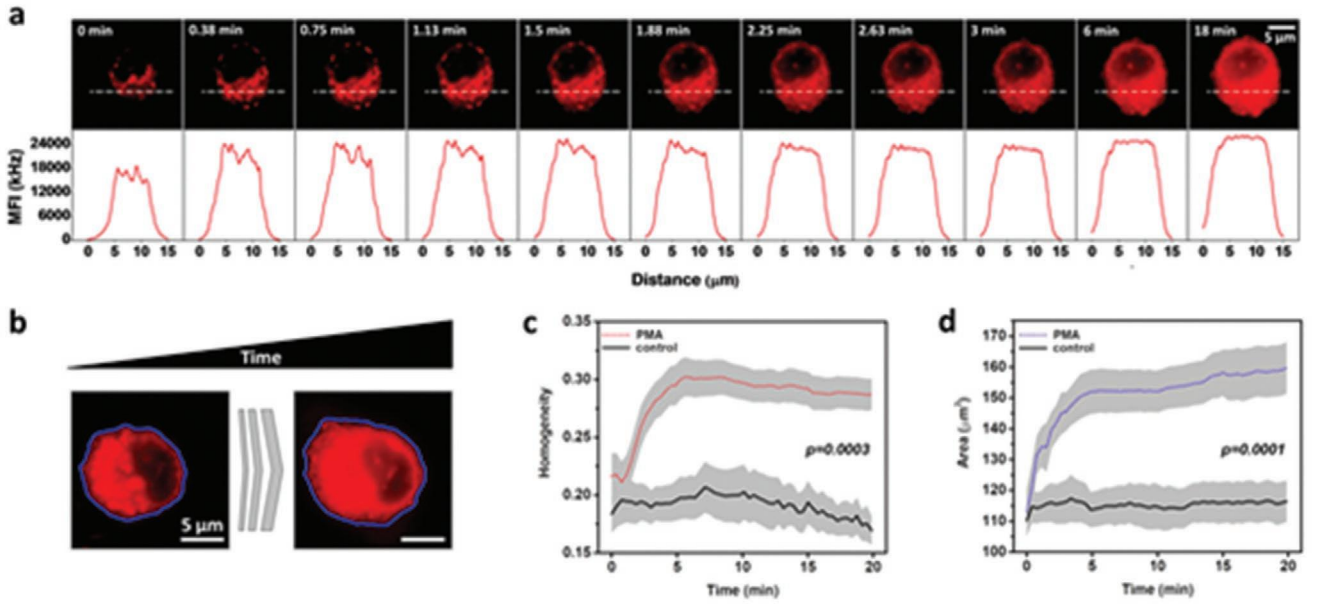

Figure 2. Reactive oxygen species (ROS) localization and morphology of optically trapped macrophages. a) Upper panel, selected time-lapse images of a phorbol 12-myristate 13-acetate (PMA) stimulated macrophage showing a fast spread of ROS signal across the cytosol. Lower panels, mean fluorescence intensity obtained from the cross-sections presented in the upper panel (dashed white lines in upper panels). The intensity profiles show heterogeneous distributions of ROS at early time points, which rapidly evolves to a well distributed cytosolic signal within the first few minutes (lower panel). b) Images of a macrophage at an early (left) and late (right) time point of the activation experiment. Blue lines represent the calculated cell contours generated by analyzing the recorded ROS signal. c) Homogeneity of the fluorescent signal calculated for the area contained within the contour shown in (b). Lines represent the average curve obtained for PMA-stimulated cells (red) and controls (black). Difference in area under the curve statistically tested with a Mann–Whitney *U* test ($p = 0.0003$). d) Average area of PMA-stimulated cells (blue) and controls (black), calculated based on the cell contours as shown in panel (b) difference in area under the curve statistically tested with a Mann–Whitney *U* test ($p = 0.0001$). Gray shades represent SEM for both PMA-stimulated ($N = 13$) and control ($N = 11$) macrophages. The analyses in b–d were performed using ICY software.[22]

uniform distribution. The PMA-stimulated macrophages displayed a fast increase in homogeneity within the first 5 min, whereas the non-stimulated cells showed lower values of homogeneity during the entire experiment (Figure 2c). Homogeneity levels were significantly higher in the PMA-stimulated macrophages, supporting the previous observations of cluster formation (Figure 2a) by ROS in the early stages of activation.

Analysis of the cell contours indicated an increase in the cell area of approximately 50% upon PMA activation (Figure 2d), which is presumably associated with a proportional change in cell volume. Simultaneously, a significant increase in cell perimeter was detected (Figure S2a, Supporting Information). These substantial changes in cell size are even appreciable by inspecting the images presented in Figure 2b. The control macrophages did not show detectable changes in cell size (Figure 2d). However, it has to be noted that we are tracking exclusively the ROS signal, which is not a direct measurement of the cell size. Although ROS saturated the cytosol at long activation times (more than 5 min), we expect that this parameter might be slightly affected by our analysis at earlier time points, as well as for control macrophages. Nonetheless, PMA has been described to increase cell size before, supporting our observations.[21] Other morphological parameters, such as roundness and sphericity, did not show any significant changes during activation (Figure S2, Supporting Information).

To summarize this part, single-cell activation experiments showed a spread of ROS clusters in the cytosol until a homogeneous distribution was reached simultaneously with a significant increase in cell size. Overall, these findings highlight the fast changes and complex behavior that macrophages adopt upon activation and the capability of our approach to visualize and analyze this behavior.

2.3. Flow Cytometry Displays Different Kinetics of PMA-Induced ROS Production

In order to verify the results obtained with our optical tweezers method, we studied the early kinetics of PMA-induced ROS production by flow cytometric analysis. Macrophages were stimulated and incubated with PMA inside flow cytometry tubes. PMA-stimulation resulted in higher intracellular ROS levels in the macrophages compared to the unstimulated macrophages (**Figure 3**a). These higher ROS levels were already observed 10 min after stimulation, the earliest time point due to sample handling time. The highest ROS levels were observed after 20 min, indicating a slower response compared to optically trapped macrophages (Figure 1d). Some technique-related aspects in the flow cytometry set-up, such as cell–cell contact and cell adhesion, could contribute to this difference as these factors do not play a role in our optical tweezers approach. However, in both cases the maximum increase in ROS levels was approximately two-fold, suggesting that the magnitude of the oxidative stress response is comparable and that only the kinetics are different (Figures 1e and 3a).

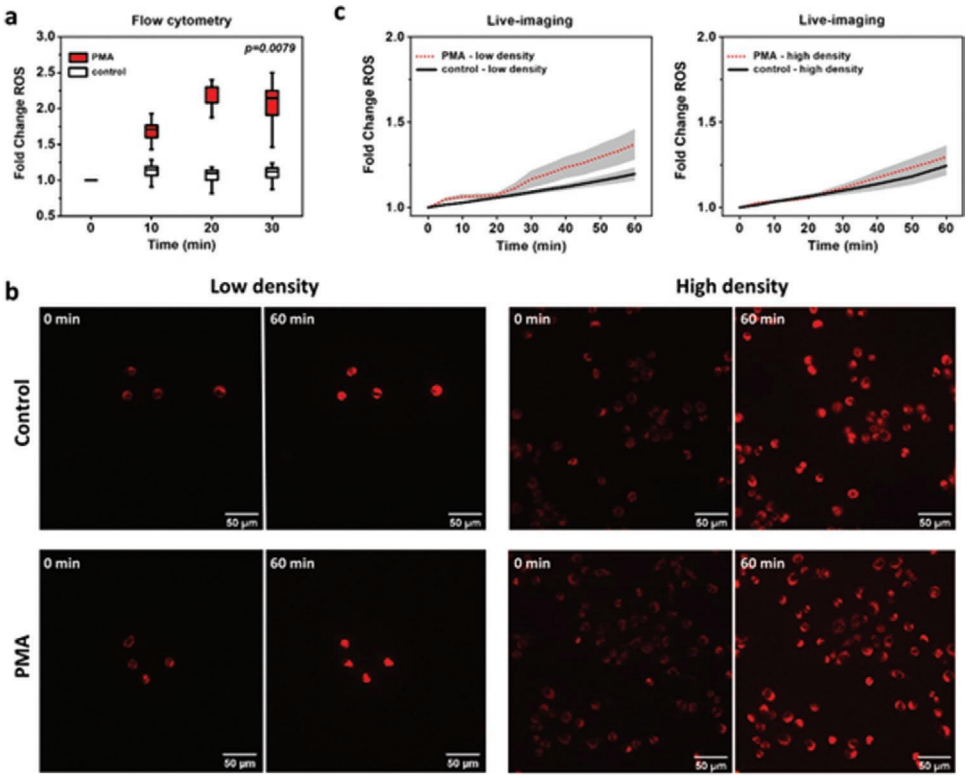

Figure 3. Effect of PMA-stimulation on reactive oxygen species (ROS) levels in RAW264.7 macrophages, as determined by flow cytometry and live-cell fluorescence imaging. a) Flow cytometry – Single-cell suspensions of RAW264.7 macrophages were stained and incubated in flow cytometry tubes. ROS levels were visualized using CellROX Deep Red reagent and measured 0, 10, 20, and 30 min after PMA-stimulation. Data displayed as min to max box-and-whiskers plots ± SEM, normalized to the ROS levels at $t = 0$ min. Difference in area under the curve statistically tested with a Mann–Whitney U test ($p = 0.0079$, $N = 5$). b) Live-cell fluorescence imaging – Attached RAW264.7 macrophages at two different densities were stained and incubated with CellROX Deep Red in a cell culture dish. ROS levels were measured every 5 min up to 60 min after stimulation with PMA. Representative images of macrophages in the four different conditions, at $t = 0$ and $t = 60$ min. c) Live-cell fluorescence imaging – Fold change in ROS levels over time in low and high cell seeding densities, respectively. Data displayed as mean fold change ± SEM (gray shades). Differences in area under the curve were tested with a Kruskal–Wallis test (NS, $N = 5$).

2.4. Macrophage Adhesion Affects the Kinetics of PMA-Induced ROS Upregulation

To investigate whether cell adhesion and cell density indeed affect the macrophage response to PMA, we performed widefield live-cell fluorescence imaging. Macrophages were seeded in glass-bottom petri dishes at low or high density and allowed to adhere for 24 h, followed by staining with CellROX Deep Red. PMA was added after making images on fixed positions to determine the baseline ROS levels ($t = 0$ min). Images were then obtained every 5 min up to 60 min (Figure 3b). No significant differences in ROS levels were found between PMA-stimulated cells and control cells, at both low and high seeding density (Figure 3c). However, there was a slight trend toward increasing ROS levels starting 20 min after stimulation with PMA and this trend was more pronounced in macrophages seeded at low density. Interestingly, a slight increase in ROS levels over time was observed in all conditions, including the unstimulated macrophages (Figure 3c). This is likely caused by the well-known phenomenon of light-induced ROS production, which is enhanced in widefield fluorescence microscopy compared to confocal fluorescence microscopy.[23,24] Compared to the results obtained by optical tweezers and flow cytometry, the response of macrophages to PMA seems to be slower when the macrophages are attached on a surface. Furthermore, the magnitude of the oxidative stress response seems to be affected as no significant increases in ROS levels were detected, even after extending the imaging time up to 60 min.

3. Discussion

We showed that optical tweezers in combination with microfluidics and confocal fluorescence microscopy is a powerful method to investigate the early kinetics of macrophage activation at the single-cell level in real-time. The optical tweezers set-up allowed us to image a fast increase in ROS levels in RAW264.7 macrophages upon stimulation with PMA, as well as changes in subcellular ROS localization and cell size. Interestingly, kinetic studies by flow cytometry and live-fluorescence imaging suggested slower and/or smaller oxidative stress responses compared to our optical tweezers method. While high intensity trapping lasers cause serious damage to cells (Figure 1f), our results under low intensity laser conditions show that ROS production kinetics is not altered, indicating that there is no measurable effect of possible heating or

radiation damage due to direct cell trapping (Figures 1 and 3). It is otherwise likely that these kinetic changes are caused by the different levels of cell–cell communication and cell adhesion that are associated with these distinct methods.

In our optical tweezers set-up, we study the response of a single macrophage without any cell–cell contact or cell–cell communication through paracrine signaling. Flow cytometry and live-fluorescence imaging do allow cell–cell contact and communication through soluble mediators. It is not unlikely that the presence of other macrophages and their secretome affect the kinetics of macrophage activation.[25] Xue et al. previously described that paracrine signaling is required for the attenuation of a pro-inflammatory macrophage response through an IL-10-mediated inhibitory feedback loop.[25] IL-10 has been shown to exert its anti-inflammatory effect on macrophages by reducing the amount of ROS produced upon a pro-inflammatory stimulus.[26] It is therefore not unlikely that a reduction in paracrine IL-10 signaling contributes to the augmented oxidative stress response in PMA-stimulated, optically trapped macrophages.

The varying levels of cell adhesion may also contribute to the kinetic differences observed between the methods. Optically trapped macrophages are in suspension, whereas macrophages are fully adhered to a surface during live-cell fluorescence imaging. Although macrophages are also suspended for flow cytometric analysis, adhesion of macrophages to the wall of the tube cannot be prevented completely. Biophysical stimuli coming from the stiff tube wall or cell culture dish may therefore interfere with macrophage responses.[7] In addition, macrophage attachment contributes to a higher degree of spatial confinement, as described by Jain et al.[27] Prevention of cell spreading (by micro patterning or cell crowding) can suppress inflammatory responses of macrophages. In our experiments, a higher degree of spatial confinement is indeed accompanied by a delayed oxidative stress response to PMA. Furthermore, adhesion of macrophages to a surface dramatically decreases the cell surface area that is exposed to the activating stimulus. This may also contribute to the accelerated oxidative stress response in trapped macrophages, as their membrane is fully exposed to the PMA.

The method presented here provides several advantages over the conventional methods to study macrophage polarization. First, it allows us to study the response of single macrophages. We can therefore investigate the heterogeneity of macrophage activation, but also prevent cell–cell cross-talk that may influence responses. Second, the optical tweezers set-up yields data with a very high resolution, both spatial and temporal. The same levels of spatial and temporal resolution can be achieved with other techniques, but simultaneously is generally challenging. However, the most important benefit of the optical tweezers approach is that we can take away the modulating effect of biophysical stimuli coming from a surface or cell–cell interactions. That way, it is possible to study the effect of one single biochemical stimulus. Expanding the optical tweezers set-up by adding extra trapping lasers will allow the introduction of various biophysical stimuli to the macrophages in a controlled manner.

In conclusion, we showed that optical tweezers can be applied to study early stage macrophage responses on a single-cell level with high spatiotemporal resolution. The deviations that are observed compared to conventional techniques emphasize the ability of cell culture conditions to interfere with in vitro macrophage responses. Our optical tweezers-based approach yields new insights in the response of macrophages to single biochemical or biophysical stimuli and thereby contributes to the much-desired better understanding of macrophage polarization.

4. Experimental Section

Macrophage Culture, Staining, and Stimulation: RAW264.7 macrophages (ATCC TIB-71) were cultured in high glucose DMEM containing GlutaMAX and sodium pyruvate, supplemented with 10% heat-inactivated FBS, 2×10^{-3} M L-Glutamine and 10 μg mL^{-1} gentamicin (Gibco Laboratories, Grand Island, USA) in an incubator at 37 °C and 5% CO_2. Cultures were reseeded twice a week at a density of 2×10^4 cells cm^{-2}, after detaching by careful scraping. RAW264.7 macrophages were used for experiments between passage number 8 and 12. Before the start of each experiment, macrophages were stained in Live Cell Imaging Solution containing 5×10^{-6} M CellROX Deep Red Reagent (Invitrogen, Carlsbad, CA, USA) for 30 min at 37 °C. Macrophages were stimulated with 16×10^{-6} M phorbol 12-myristate 13-acetate (PMA) (Sigma-Aldrich, Zwijndrecht, The Netherlands) and unstimulated macrophages were included as control.

Optical Tweezers Set-Up with Confocal Fluorescence Microscopy: The dual-trap optical tweezers with 3-color confocal fluorescence microscopy set-up[28] (C-trap, LUMICKS, Amsterdam, The Netherlands), was used for the single-cell kinetic experiments. A 5-channel microfluidic cell (LUMICKS) mounted on an automated XY-stage was used to isolate individual cells under different conditions. The microfluidic cell was coated with BSA (0.1% w/v) and Pluronic F127 (0.5% w/v) solutions to avoid cell adhesion. Cell trapping was performed by a 1064 nm wavelength laser with maximum output power of ≈10 W. Fluorescence images were generated by scanning the confocal volume over a region of 20 × 20 μm at 2.6 frames min^{-1}. Excitation was performed by 532 and 638 nm wavelength lasers at ≈1 and ≈7 μW, respectively. Fluorescence emission was recorded by single photon counters (Avalanche Photodetectors, APDs).

Cell Trapping and Kinetic Measurements of Macrophage Activation: A suspension of 0.5×10^6 cells mL^{-1} in live-cell imaging solution was flushed into the microfluidic cell. The solution was supplemented with 0.1% w/v Pluronic F127 and 5×10^{-3} M EDTA (Sigma-Aldrich) to avoid cells sticking to the microfluidic system. In the absence of flow, cells were trapped using a dual beam separated by 2 nm 10% laser power (<50 mW). With these settings, cells were isolated by moving to a different channel in the microfluidic cell for activation and imaging in the absence of Pluronic F127 and EDTA. Once in the activation channel, the trapping laser power was lowered 10 times (1% laser power) prior to measurements. Cell viability was monitored in real time by adding 125×10^{-9} M SYTOX Orange (Invitrogen) to the live cell imaging solution. The dynamic stain of nucleic acids by SYTOX has demonstrated its suitability for continuous imaging applications over temporal scales of minutes to hours.[29,30] Cell stimulation was carried out with 16×10^{-6} M PMA, and 5×10^{-6} M CellROX Deep Red Reagent was added to follow the ROS signal. Control experiments were carried out under the same conditions, but in the absence of PMA.

Flow Cytometry: For flow cytometric analysis, macrophages were seeded into flow cytometry tubes at a concentration of 2×10^6 cells mL^{-1}. PMA-stimulated and unstimulated samples were measured with a CytoFLEX S Flow Cytometer (Beckman Coulter, Woerden, The Netherlands) 0, 10, 20 and 30 min after addition of PMA. Data analysis was performed using FlowJo Software (Tree Star, Ashland, OR, USA). An example of the gating strategy is shown in Figure S3 (Supporting Information).

Live-Cell Fluorescence Microscopy: RAW264.7 macrophages were seeded in a CELLview glass bottom petri dish (Greiner Bio-One, Alphen

aan den Rijn, The Netherlands) at a density of 0.91×10^5 cells cm^{-2} (high density) or 0.91×10^3 cells cm^{-2} (low density). After 24 h, the cell culture medium was replaced with live-cell imaging solution containing 5×10^{-6} M CellROX Deep Red Reagent. After 30 min incubation at 37 °C, macrophages were stimulated with 16×10^{-6} M PMA or not stimulated (control). Fluorescence and bright-field images were obtained at 37 °C on fixed positions with a DeltaVision Elite microscope (GE Healthcare, IL, United States) every 5 min, up to 1 h after stimulation.

Image Analysis: Mean fluorescence intensities were extracted from the fluorescence microscopy images using Fiji.[31] Cell contours for the CellROX channel were calculated by applying the 2-D meshes plug-in.[32] Further quantification of the morphological parameters such as perimeter, area, sphericity, roundness, and homogeneity were performed by the ROI statistics plug-in build in ICY software.[22] Explicitly, homogeneity is defined as the inverse difference moment, from 0 to 1, based on Haralick texture features.[33]

Statistical Analysis: Kinetic differences were quantified by calculating the area under the curve (AUC) of the normalized data, followed by statistical testing as indicated per graph to detect significant differences ($p < 0.05$). Statistical analyses were performed in GraphPad Prism 8.0 (GraphPad Software, La Jolla, CA, USA).

Supporting Information

Supporting Information is available from the Wiley Online Library or from the author.

Acknowledgements

G.F.V. and P.B. contributed equally to this work. This study was supported by the Graduate School of Medical Sciences of the University Medical Center Groningen (to G.F.V. and P.v.R) and the UMCG Imaging and Microscopy Center (UMIC), where part of the work has been performed. W.H.R was supported by a VIDI grant from the Nederlandse Organisatie voor Wetenschappelijk Onderzoek (NWO).

Conflict of Interest

The authors declare the following competing financial interest(s): P.v.R. is co-founder, scientific advisor, and shareholder of BiomACS BV, a biomedical-oriented screening company.

Data Availability Statement

Research data are not shared.

Keywords

early kinetics, optical tweezers, oxidative stress response

Received: September 11, 2020
Revised: January 27, 2021
Published online:

[1] P. J. Murray, *Annu. Rev. Physiol.* **2017**, *79*, 541.
[2] P. J. Murray, J. E. Allen, S. K. Biswas, E. A. Fisher, D. W. Gilroy, S. Goerdt, S. Gordon, J. A. Hamilton, L. B. Ivashkiv, T. Lawrence, M. Locati, A. Mantovani, F. O. Martinez, J. L. Mege, D. M. Mosser, G. Natoli, J. P. Saeij, J. L. Schultze, K. A. Shirey, A. Sica, J. Suttles, I. Udalova, J. A. van Ginderachter, S. N. Vogel, T. A. Wynn, *Immunity* **2014**, *41*, 14.
[3] D. Aran, A. P. Looney, L. Liu, E. Wu, V. Fong, A. Hsu, S. Chak, R. P. Naikawadi, P. J. Wolters, A. R. Abate, A. J. Butte, M. Bhattacharya, *Nat. Immunol.* **2019**, *20*, 163.
[4] J. Xue, S. V. Schmidt, J. Sander, A. Draffehn, W. Krebs, I. Quester, D. DeNardo, T. D. Gohel, M. Emde, L. Schmidleithner, H. Ganesan, A. Nino-Castro, M. R. Mallmann, L. Labzin, H. Theis, M. Kraut, M. Beyer, E. Latz, T. C. Freeman, T. Ulas, J. L. Schultze, *Immunity* **2014**, *40*, 274.
[5] N. Jain, J. Moeller, V. Vogel, *Annu. Rev. Biomed. Eng.* **2019**, *21*, 267.
[6] F. O. Martinez, S. Gordon, *F1000Prime Rep.* **2014**, *6*, 13.
[7] V. S. Meli, P. K. Veerasubramanian, H. Atcha, Z. Reitz, T. L. Downing, W. F. Liu, *J. Leukocyte Biol.* **2019**, *106*, 283.
[8] S. Gordon, A. Plüddemann, *BMC Biol.* **2017**, *15*, 53.
[9] T. Ravasi, C. Wells, A. Forest, D. M. Underhill, B. J. Wainwright, A. Aderem, S. Grimmond, D. A. Hume, *J. Immunol.* **2002**, *168*, 44.
[10] A. Sica, A. Mantovani, *J. Clin. Invest.* **2012**, *122*, 787.
[11] S. Gupta, A. R. Dinasarapu, M. J. Gersten, M. R. Maurya, S. Subramaniam, in *Macrophages: Biology and Role in the Pathology of Diseases*, (Eds.: S. K. Biswas, A. Mantovani) Springer, New York **2014**, p. 587.
[12] A. Ashkin, J. M. Dziedzic, *Science* **1987**, *235*, 1517.
[13] M. Hashemi Shabestari, A. E. C. Meijering, W. H. Roos, G. J. L. Wuite, E. J. G. Peterman, *Methods Enzymol.* **2017**, *582*, 85.
[14] E. Eriksson, J. Enger, B. Nordlander, N. Erjavec, K. Ramser, M. Goksör, S. Hohmann, T. Nyström, D. Hanstorp, *Lab Chip* **2007**, *7*, 71.
[15] M. Werner, F. Merenda, J. Piguet, R. P. Salathé, H. Vogel, *Lab Chip* **2011**, *11*, 2432.
[16] D. Wolfson, M. Steck, M. Persson, G. Mcnerney, A. Popovich, M. Goksör, T. Huser, *J. Biophotonics* **2015**, *8*, 208.
[17] S. Fore, J. Chan, D. Taylor, T. Huser, *J. Opt.* **2011**, *13*, 044021.
[18] H. Zhang, K. K. Liu, *J. R. Soc., Interface* **2008**, *5*, 671.
[19] J. Gieche, J. Mehlhase, A. Licht, T. Zacke, N. Sitte, T. Grune, *Biochim. Biophys. Acta, Mol. Cell Res.* **2001**, *1538*, 321.
[20] K. Zhao, Z. Huang, H. Lu, J. Zhou, T. Wei, *Biosci. Rep.* **2010**, *30*, 233.
[21] M. Daigneault, J. A. Preston, H. M. Marriott, M. K. B. Whyte, D. H. Dockrell, *PLoS One* **2010**, *5*, e8668.
[22] F. De Chaumont, S. Dallongeville, N. Chenouard, N. Hervé, S. Pop, T. Provoost, V. Meas-Yedid, P. Pankajakshan, T. Lecomte, Y. L. Montagner, T. Lagache, A. Dufour, J. C. Olivo-Marin, *Nat. Methods* **2012**, *9*, 690.
[23] C. Boudreau, T. L. Wee, Y. R. Duh, M. P. Couto, K. H. Ardakani, C. M. Brown, *Sci. Rep.* **2016**, *6*, 30892.
[24] J. Icha, M. Weber, J. C. Waters, C. Norden, *BioEssays* **2017**, *39*, 1700003.
[25] Q. Xue, Y. Lu, M. R. Eisele, E. S. Sulistijo, N. Khan, R. Fan, K. Miller-Jensen, *Sci. Signaling* **2015**, *8*, ra59.
[26] S. Dokka, X. Shi, S. Leonard, L. Wang, V. Castranova, Y. Rojanasakul, *Am. J. Physiol.: Lung Cell. Mol. Physiol.* **2001**, *280*, L1196.
[27] N. Jain, V. Vogel, *Nat. Mater.* **2018**, *17*, 1134.
[28] M. Marchetti, D. Kamsma, E. Cazares Vargas, A. Hernandez García, P. Van Der Schoot, R. De Vries, G. J. L. Wuite, W. H. Roos, *Nano Lett.* **2019**, *19*, 5746.
[29] A. E. C. Meijering, A. S. Biebricher, G. Sitters, I. Brouwer, E. J. G. Peterman, G. J. L. Wuite, I. Heller, *Nucleic Acids Res.* **2020**, *48*, e34.
[30] A. S. Backer, M. Y. Lee, W. E. Moerner, *Optica* **2016**, *3*, 659.
[31] J. Schindelin, I. Arganda-Carreras, E. Frise, V. Kaynig, M. Longair, T. Pietzsch, S. Preibisch, C. Rueden, S. Saalfeld, B. Schmid, J. Y. Tinevez, D. J. White, V. Hartenstein, K. Eliceiri, P. Tomancak, A. Cardona, *Nat. Methods* **2012**, *9*, 676.
[32] A. Dufour, R. Thibeaux, E. Labruyère, N. Guillén, J. C. Olivo-Marin, *IEEE Trans. Image Process.* **2011**, *20*, 1925.
[33] R. M. Haralick, *Proc. IEEE* **1979**, *67*, 783.
[34] H. Wadell, *J. Geol.* **1935**, *43*, 250.